

# UAV CONTROLLER PERFORMANCE UNDER WIND DISTURBANCE

Muhammad Hazman Zaharuddin<sup>a</sup>, Mastura Ab Wahid<sup>a,\*</sup>, Norazila Othman<sup>a</sup>, Mohd Zarhamdy Md Zain<sup>a</sup>, Istas Fahrurrazi Nusyirwan<sup>a</sup>

<sup>a</sup> Faculty of Mechanical Engineering, Faculty of Engineering, Universiti Teknologi Malaysia, 81310 UTM Johor Bahru, Johor, Malaysia

## Article history

Received

7<sup>th</sup> October 2020

Received in revised form

5<sup>th</sup> September 2023

Accepted

5<sup>th</sup> September 2023

Published

1<sup>st</sup> December 2023

\*Corresponding author  
masturawahid@utm.my

## GRAPHICAL ABSTRACT



## ABSTRACT

In the world of Unmanned Aircraft Vehicle, controls and stability are important to ensure a safe flight mission. As UAVs are an aircraft that operates dependently to the reference trajectory given, a reliable system and controller are in need for the UAV to carry through flight missions safely. This research focusses on the design of a cascaded PID controller to control the UAV to follow climb, cruise, and landing trajectory. The designed PID is tested to see the system robustness when influenced by wind disturbances. The response of flight under influence of wind is acceptable, however, the controller does not satisfy the system's flying quality at a wind disturbance exceeding step input of 1-70 km/h and 1-100 km/h or above due to the size of the UAV. The acceptable response are accounted for final gains of  $kp_q \approx 0, ki_q \approx 0, kd_q = -0.00034, kp_\theta = -0.5116, ki_\theta = -0.002267, kd_\theta = 0, kp_h = 13.3931, ki_h = 1.01882$  and  $kd_h = 13.9178$  in order to achieve such results.

## KEYWORDS

Wind disturbance; PID controller; UAV Climb and Landing

## LIST OF ABBREVIATIONS AND SYMBOLS

UAS	-	Unmanned Aircraft System
DOF	-	Degree of Freedom
NTSB	-	National Transportation Safety Board
$\delta$	-	Deflection
$D, d$	-	Diameter
$F$	-	Force
$v$	-	Velocity
$P$	-	Pressure
$I$	-	Moment of Inertia
$r$	-	Radius
$Re$	-	Reynold Number
$T_u$	-	Period, s
$\lambda$	-	Eigenvalue
$\phi$	-	Roll
$\theta$	-	Pitch
$\psi$	-	Yaw

## INTRODUCTION

Taking off and landing are considered the most dangerous phases of a mission due to the aircraft's need to maintain its exact trajectory, velocity, and altitude since UAVs are consistently affected by model uncertainties, noises, and disturbances. As referred from [1], actual ground effect and atmospheric disturbance are unavoidable for aircraft traveling under low altitudes. The controller technique is crucial in ensuring the stability of the aircraft under these conditions. The current trend towards the increased use of Unmanned Aircraft

Vehicles (UAVs) has spiked, particularly regarding usage in military applications. In order to ensure a stable and effective flight mission, a robust and reliable controller must be added to the system, as deployment of UAVs will not always be prudent in favor of weather and windy conditions.

The equation of motion for flying vehicles is based on two commonly used techniques: the Euler-Lagrange method or Newton’s approach. Based on Newton’s Second law states that the summation of all external forces acting on a body is equal to the time rate of change of the momentum of the body, and the summation of the external moment acting on a body is equal to the time rate of change of the angular momentum. These equations deduced the relationship between forces in the body frame ( $F_x, F_y, F_z$ ), moments ( $L, M, N$ ), linear velocities ( $u, v, w$ ) and angular velocities ( $p, q, r$ ). Through small disturbance theory, the motion of airplane is assumed to consist of the equation of motion plus the perturbation or disturbance.

The aerodynamic forces and moments are expressed through perturbation variable using Taylor’s series [2]. Assuming the equations have a nominal value at trimmed flight, the changes of each force and moments elements ( $\Delta X, \Delta Y, \Delta Z, \Delta L, \Delta M, \Delta N$ ) are produced as the results of change in ( $u, v, w, \delta, p, q, r$ ). Due to  $Z_{\dot{w}}$  and  $Z_{\dot{\omega}}$  being too small and insignificant, they are neglected and hence, giving the longitudinal motion of state-space form equation to be,

$$\begin{bmatrix} \Delta \dot{u} \\ \Delta \dot{w} \\ \Delta \dot{q} \\ \Delta \dot{\theta} \end{bmatrix} = \begin{bmatrix} X_u & X_w & 0 & -g \\ Z_u & Z_w & u_0 & 0 \\ M_u + M_w Z_u & M_w + M_w Z_w & M_q + M_w u_0 & 0 \\ 0 & 0 & 1 & 0 \end{bmatrix} \begin{bmatrix} \Delta u \\ \Delta w \\ \Delta q \\ \Delta \theta \end{bmatrix} + \begin{bmatrix} X_{\delta_e} & X_{\delta_r} \\ Z_{\delta_e} & Z_{\delta_r} \\ M_{\delta} + M_w Z_{\delta} & M_{\delta_r} + M_w Z_{\delta_r} \\ 0 & 0 \end{bmatrix} \begin{bmatrix} \Delta \delta_e \\ \Delta \delta_r \end{bmatrix} \quad (1)$$

The derivatives of the state-space equations were given as follows: When represented mathematically,

$$\dot{x} = Ax + B\eta$$

Where  $x$  is the state vector,  $\eta$  is the control vector, and matrices  $A$  and  $B$  contain the aircraft dimensional stability derivatives.

The atmosphere contains many aircraft motion disturbances and is usually characterized by wind, gusts, and turbulence. Ever since the creation of flight, statistics have proven that a considerable part of flight accidents occur due to unfavorable atmospheric disturbances. According to [1,9], it was stated that a few of the wind-resulting accidents

can be categorized as wake vortex, downburst, wind shear, and wind turbulence. As for the UAV’s perspective, they are more susceptible to wind disturbance due to their size, weight, lower flight speed, and altitude factors.

The forces and moments need to be related to the relative of motion and with respect to the atmosphere.

As the aerodynamic forces and moments on the aircraft depend on the relative motion of the aircraft to the atmosphere, the use of forces and moments of atmospheric disturbances such as wind, gust, and turbulence must be related to the relative movement of the atmosphere. The equation of motion with account for atmospheric disturbances can be written in the state-space form as,

$$\dot{x} = Ax + B\eta + C\xi$$

$x$  is the state,  $\eta$  is the control, and  $\xi$  is the gust disturbance vectors. Hence, the longitudinal equation (1) has been deduced in [5].

$$\begin{bmatrix} \Delta \dot{u} \\ \Delta \dot{w} \\ \Delta \dot{q} \\ \Delta \dot{\theta} \end{bmatrix} = \begin{bmatrix} X_u & X_w & 0 & -g \\ Z_u & Z_w & u_0 & 0 \\ M_u & M_w & M_q & 0 \\ 0 & 0 & 1 & 0 \end{bmatrix} \begin{bmatrix} \Delta u \\ \Delta w \\ \Delta q \\ \Delta \theta \end{bmatrix} + \begin{bmatrix} X_{\delta_e} & X_{\delta_r} \\ Z_{\delta_e} & Z_{\delta_r} \\ M_{\delta_e} & M_{\delta_r} \\ 0 & 0 \end{bmatrix} \begin{bmatrix} \Delta \delta_e \\ \Delta \delta_r \end{bmatrix} + \begin{bmatrix} -X_u & -X_w & 0 \\ -Z_u & -Z_w & 0 \\ -M_u & -M_w & -M_q \\ 0 & 0 & 1 \end{bmatrix} \begin{bmatrix} U_g \\ W_g \\ q_g \end{bmatrix} \quad (2)$$

According to [3], the reference wind speed used in most construction codes is recorded at a height of 10m, but wind speed increases as height increases. The wind speed profile can be modeled by power law, as shown in equation (3). The exponential variation of wind speed with height can be defined as follows

$$U_g = \frac{dU}{dh} dh \text{ and } \frac{dU}{dh} = \zeta \frac{U(h)}{h} \quad (3)$$

Where  $\zeta$  is the surface roughness typically from 0.08 to 0.52 and  $U(h)$  wind speed at height  $h$ . The standard peak wind speed value obtained from the [4] is stated to be between the range of 100 to 120 km/hr, recorded at 10m of height. In this research, the designed controller has been tested with four (4) different wind values to evaluate the performance of the controller.

## METHODOLOGY

This research is fully MATLAB-dependent in calculation, simulation, and visualization. The model of the UAV is CAMAR UTM. Extracted from

the aerodynamic forces and moments and only considering the input from the elevators, the equations are expressed in means of perturbation variable using Taylor’s series to form the equation of linear state space longitudinal equation,

$$\begin{bmatrix} \Delta \dot{u} \\ \Delta \dot{w} \\ \Delta \dot{q} \\ \Delta \dot{\theta} \end{bmatrix} = \begin{bmatrix} X_u & X_w & 0 & -g \\ Z_u & Z_w & u_o & 0 \\ M_u + M_{\dot{w}}Z_u & M_w + M_{\dot{w}}Z_w & M_q + M_{\dot{w}}u_o & 0 \\ 0 & 0 & 1 & 0 \end{bmatrix} \begin{bmatrix} \Delta u \\ \Delta w \\ \Delta q \\ \Delta \theta \end{bmatrix} + \begin{bmatrix} X_{\delta_e} & X_{\delta_T} \\ Z_{\delta_e} & Z_{\delta_T} \\ M_{\delta} + M_{\dot{w}}Z_{\delta} & M_{\delta_T} + M_{\dot{w}}Z_{\delta_T} \\ 0 & 0 \end{bmatrix} [\Delta \delta e] \quad (4)$$

From Equation (4), the eigenvalues are presented in order to determine the phugoid and short-period calculation of period and cycle. The approximation method is then carried out by rewriting and solving equation (4) to produce the approximation of phugoid and short period as tabulated in table 1,

**Table 1:** Longitudinal approximation in terms of damping and frequency [5]

	Long period (phugoid)	Short period
Frequency	$\omega_{np} = \frac{\sqrt{-Z_u g}}{u_o}$	$\omega_{nsp} = \frac{\sqrt{Z_{\alpha} M_q - M_{\alpha}}}{u_o}$
Damping Ratio	$\zeta_p = \frac{-X_u}{2\omega_{np}}$	$\zeta_{sp} = \frac{M_q + M_{\alpha} + \frac{Z_{\alpha}}{u_o}}{2\omega_{nsp}}$

The eigenvalue and approximation methods are compared to indicate the better mode between

phugoid and short period. The stability derivatives can be determined by comparing the frequency and damping ratio of the longitudinal response and the general design data of longitudinal flying qualities [7,8].

**Table 2:** Design objective

	Settling time	overshoot	Steady-state error
$q$	< 10s	< 2%	< 0.5%
$\theta$	< 30s	< 2%	< 0.5%
$h$	< 50s	< 5%	< 0.5%

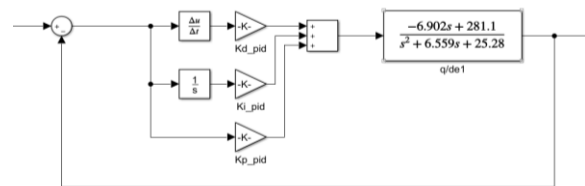


**Figure 1:** Implementation of PID to inner loop system

Based on figure 1, the inner dynamics of the system based on the approximation equation have been calculated, and the inner controller has been designed from the resultant of the step response and root locus analysis. The results are then compared to the design objectives.

A cascaded controller of pitch angle controller and altitude controller are tuned respectively through means of iteration process as shown in figure 2. The starting controller has been tuned from the inner loop, followed by the outer loop. The resultant system is then compared with the design reference objective.

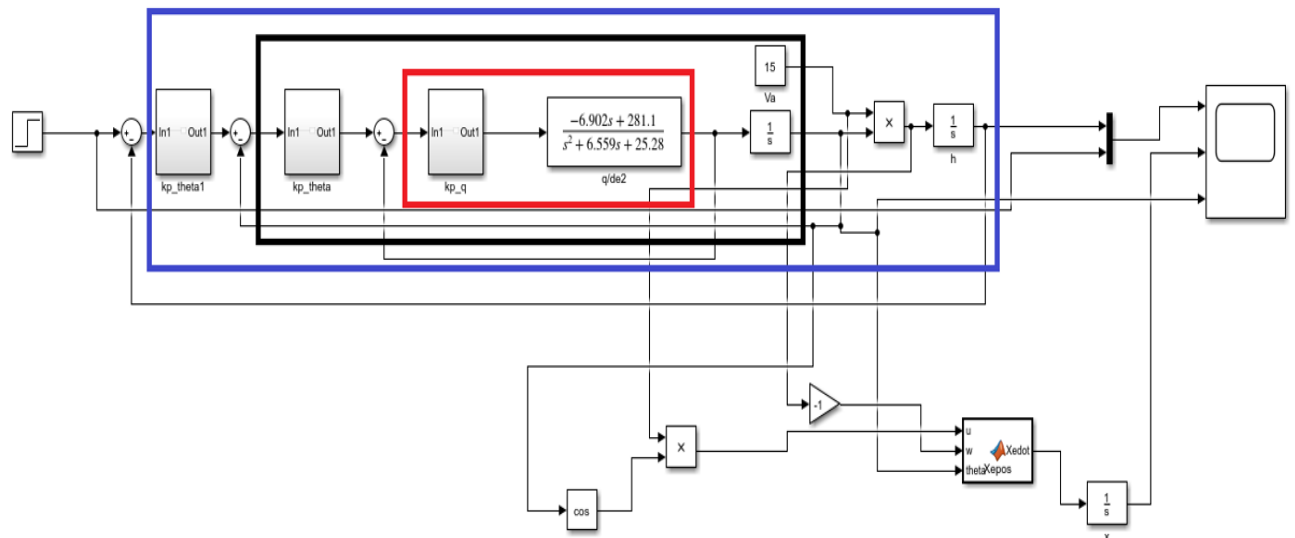


**Figure 2:** Simulink structure of closed loop with controllers

Next, the system is run through two (2) conditions of flight mission, as shown in Figure 3. Figure 3(a) shows a normal take-off and landing and a modified mission path objectively to reduce flare effects during landing, as shown in Figure 3(b). Based on the graph, for a normal flight, the UAV is set to take off at 50sec up to an altitude of 10m, then cruising from 50sec to 450sec before landing. Figure 3(b) shows that the aircraft changes its altitude at 270sec from 10m to 5m before landing to reduce the flare effect. The findings are studied on the system's overshoot, settling time, and state error.

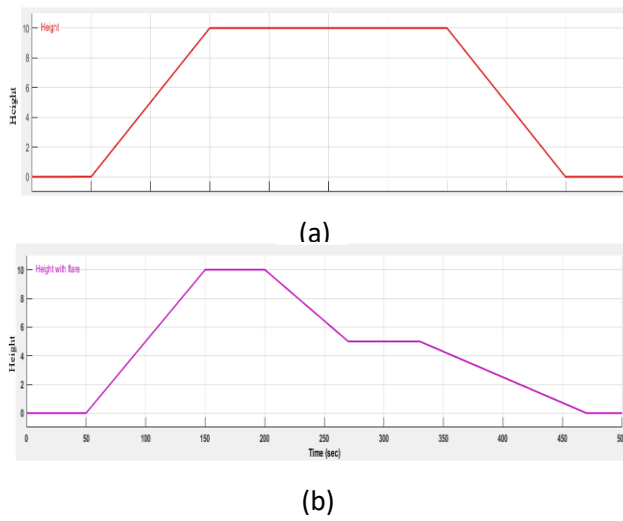


**Figure 3:** Signal Builder configuration (a) normal configuration (b) flare configuration

Lastly, the system is studied when wind disturbance has been implemented. Through the expression of gust field, the atmosphere has been defined in gust components such as in equation (5) where only the effect of wind is on the horizontal axis that is  $u_g$  as shown below.

$$\begin{bmatrix} \Delta \dot{u} \\ \Delta \dot{w} \\ \Delta \dot{q} \\ \Delta \dot{\theta} \end{bmatrix} = \begin{bmatrix} X_u & X_w & 0 & -g \\ Z_u & Z_w & u_0 & 0 \\ M_u & M_w & M_q & 0 \\ 0 & 0 & 1 & 0 \end{bmatrix} \begin{bmatrix} \Delta u \\ \Delta w \\ \Delta q \\ \Delta \theta \end{bmatrix} + \begin{bmatrix} X_{\delta_e} & X_{\delta_T} \\ Z_{\delta_e} & Z_{\delta_T} \\ M_{\delta_e} & M_{\delta_T} \\ 0 & 0 \end{bmatrix} \begin{bmatrix} \Delta \delta_e \\ \Delta \delta_T \end{bmatrix} + \begin{bmatrix} -X_u & -X_w & 0 \\ -Z_u & -Z_w & 0 \\ -M_u & -M_w & -M_q \\ 0 & 0 & 1 \end{bmatrix} [u_g] \quad (5)$$

The results have been evaluated from wind disturbance initial step input to final input of 1-10 km/hr, 1-30 km/hr, 1-50 km/hr, 1-70 km/hr, and 1-100 km/hr. The results are then compared to the design reference objective.

## RESULTS AND DISCUSSION

The flying quality of CAMAR [6] has been evaluated using table 1, and the result of frequency and damping is tabulated in Table 3. By referring to Table 3, the damping ratio and natural frequency have been compared to the general design data of longitudinal flying qualities, which proves to be a category B flight phase and Level 1 ( $0.3 < 0.5912 < 2.0$ ) flying quality based on the range of its damping ratio.

**Table 3:** Damping ratio and natural frequency of phugoid and short period

Phugoid	$Frequency = \omega_{np}$ $= 0.7611 \frac{rad}{s}$ $Damping\ ratio = \zeta_p$ $= 0.0620$
Short-period	$Frequency = \omega_{nsp} = 5.8122$ $Damping\ ratio = \zeta_{sp}$ $= 0.5912$

From the pure inner dynamic equation, the root locus and step response are indicated in Figure 4 and Figure 5,

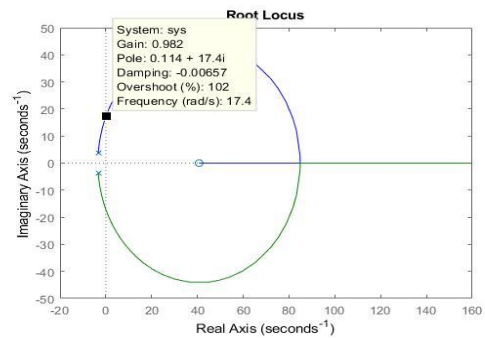


**Figure 4:** Root locus of inner dynamic

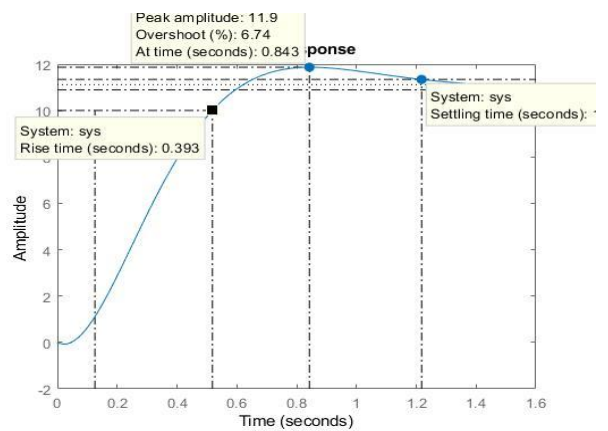


**Figure 5:** Step response of inner dynamic

As the amplitude results did not achieve the reference 1 required, a suitable controller is needed to provide stability to the system. Through root

locus, the resultant imaginary axis at  $= \pm 17.4i$ . The respondents of such axis are at  $K_{pu} = 0.982$  and period,  $T_u = \frac{2\pi}{\omega} = \frac{2\pi}{17.4} = 0.3611s$ . Hence, the gain of P, I and D are obtained below, resulting in step response in Figure 5.

$$k_p = 0.6k_{pu} = 0.5892$$

$$k_i = \frac{0.6k_{pu}}{0.5T_u} = 3.2667$$

$$k_d = 0.6k_{pu}(0.125T_u) = 0.0266$$

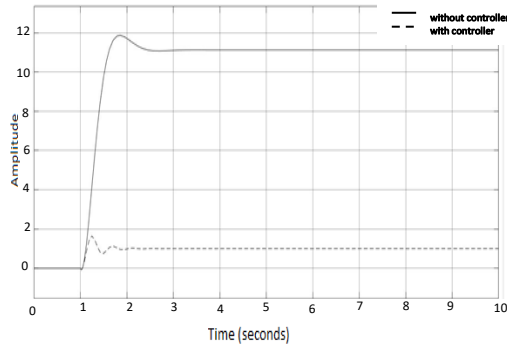


**Figure 6:** Step response of inner dynamic with and without PID controller

The controller in Figure 6 responded well towards the step response. However, there are presence of oscillation from the response with controller due to the overshoot of 62.5% and amplitude of 1.019 and settling time percentage of 32.3%. The controller is still unfavorable in terms of its massive overshoot but acceptable settling time to the design objective of  $< 10s$ .

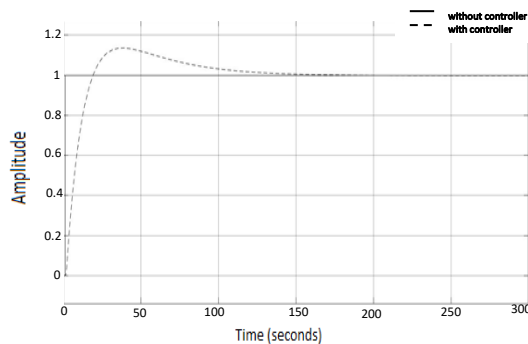


**Figure 7:** Step response with and without PID theta controller

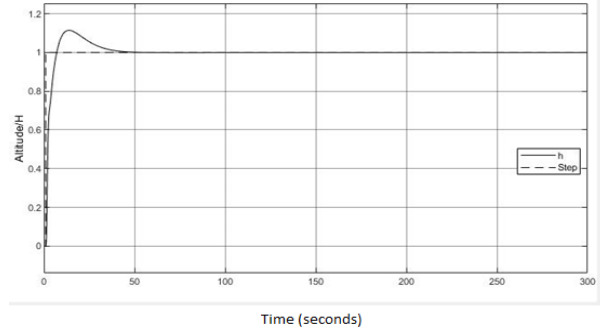


**Figure 8:** Altitude/H of system with PID controllers

From Figure 7, the response with the pitch controller reduced the oscillation of the step response with an overshoot of only 14.368% and achieved a closer range towards 1 compared to the results gain in controller at inner loop itself. It also has a faster rise time of 12.468s and a settling time percentage of 37.56%.

Referring to Figure 8, the controller achieves a much more stable and robust step response. It reduces the oscillation with an overshoot percentage of 11.798% and a settling time of 10.64%. The gain and quality of controllers can be seen in Table 4. Compared to the design objective, the overshoot does not satisfy the required objective of  $< 5\%$  but improves its settling time of  $< 50s$ . The controllers' design is still acceptable and in conjunction with the objective design required.

**Table 4:** Gain result without wind

	$k_p$	$k_i$	$k_d$	settling	overshoot
$q$	-6.14e-07	-1.72e-10	0.00034	32.3%	62.5%
$\theta$	-0.5116	-0.002267	0	37.56%	14.368%
Altitude /H	13.3931	1.0182	13.9178	10.64%	11.798%

From the modified signal builder, the normal take-off and landing from Figure 9 have an excellent response in conjunction with less or very few oscillations, with an overshoot of only 1.546% towards the signal builder. The trajectory closely follows the signal given with very few state errors. However, the results from modified take-off and landing are not that favorable in conjunction with the normal take-off and landing profile. It created a result with an overshoot percentage of 103.061%.

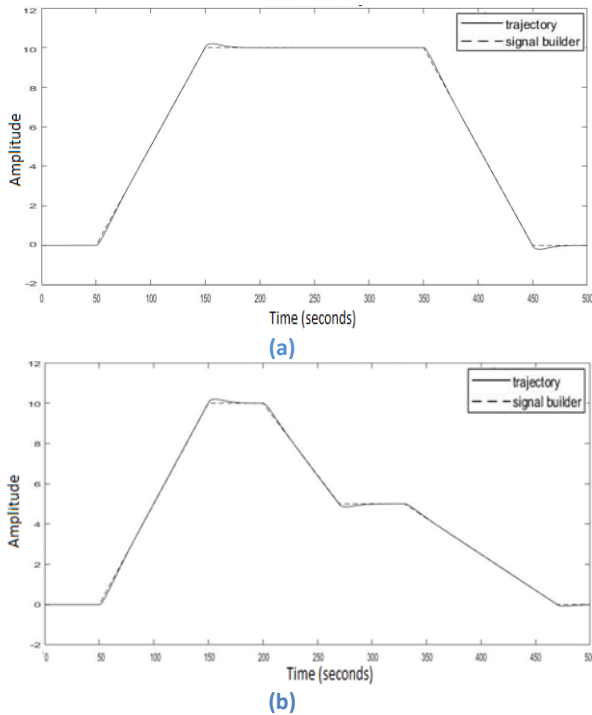


**Figure 9:** Signal Builder configuration (a) normal configuration (b) flare configuration

Moreover, the results for both signals did not counter the flare estimation well. The aircraft will experience a crash when landing due to the exceed overshoot. A well-designed flare equation needs to be implemented to the system to counteract this problem properly, rather than designing the input signal itself.

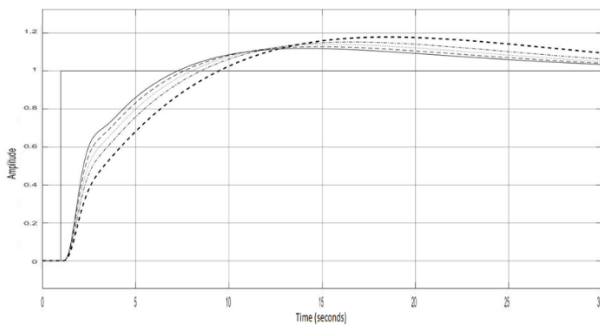


**Figure 10:** Comparison of Wind disturbance

Figure 10 indicates that the more robust input for wind disturbance will result in a lower rise time and slower trajectory of the UAV to its signal point of 1. From equation (5), a distinct input of step amplitude over  $u_o$  are calculated to measure the flight qualities of the system in such of, step input amplitude of 1-10 km/hr, 1-30 km/hr, 1-50 km/hr, 1-70 km/hr and 1-100 km/hr.

**Table 5:** Wind disturbance at different step input

Step input (km/hr)	Overshoot	Settling time
1-10	11.798%	30.5380%
1-30	13.068%	34.9684%
1-50	14.368%	39.3988%
1-70	15.698%	44.7784%
1-100	18.452%	53.6392%

From Table 5, the design objectives are still acceptable and reachable from step input 1-10 to 1-50 km/hr when compared to the design objective. The controller does not satisfy the system’s flying quality at a wind disturbance exceeding 1-70 and 1-100 km/hr or above due to its size.

## CONCLUSION

This paper discussed the design of a PID controller for the UAV to follow a reference trajectory when influenced by wind disturbance. An inner loop  $q$  controller has been constructed, followed by a cascaded PID controller of pitch angle and altitude using an iteration process. The controller design has been constructed by modifying matrix  $A$ 's eigenvalues, representing the system's poles and stability. The resultant controllers produced are compared with the design objectives specifications of overshoot and settling time and have proven acceptable.

The complete controller-equipped system is tested by implementing wind disturbance and has been validated as susceptible to the wind strength input from 1-10 to 1-50 km/hr. Step input of wind disturbance exceeding these values requires finer tuning of controllers to achieve stability on par to the design objectives proposed.

## ACKNOWLEDGEMENTS

The authors would like to acknowledge the support form Aerolab Universiti Teknologi Malaysia and financial support from UTMFR Q.J130000.2551.21H61 and Tier 1 Q.J130000.2524.20H30

## REFERENCES

[1] Wang, B. H., Wang, D. B., Ali, Z. A., Ting Ting, B. and Wang, H. (2019) ‘An overview of various kinds of wind effects on unmanned aerial vehicle’, *Measurement and Control (United Kingdom)*, 52(7–8), pp. 731–739

- [2] Høstmark, J. B. (2007) 'Modelling Simulation And Control of Fixed-Wing Uav: Cyberswan', Master's Thesis, (June), pp. 1–122.
- [3] Hamizah J 2010 Determination of Direction Factor, Md for MS 1553:2002 wind Loading for Building Structure. Faculty of Civil Engineering & Earth Resources, University Malaysia Pahang.
- [4] Malaysian Standard MS 1553: 2002 Code of Practice on Wind Loading for Building Structure, Department of Standards Malaysia
- [5] Nelson, R. C. (1998) *Flight Stability*.
- [6] Mansor, S., Ab Han, M.A. and Nasir, M.N.M., 2020. FLIGHT DYNAMICS AND CONTROL OF A V-TAIL CAMAR UAV. *Journal of Transport System Engineering*, pp.12-32.
- [7] Elsayed, A., Hafez, A., Ouda, A. N., Ahmed, H. E. H. and Abd-Elkader, H. M. (2015) 'Design of Longitudinal Motion Controller of a Small Unmanned Aerial Vehicle', *International Journal of Intelligent Systems and Applications*, 7(10), pp. 37–47.
- [8] Poksawat, P. (2018) 'Control System for Fixed-wing Unmanned Aerial Vehicles: Automatic Tuning, Gain Scheduling, and Turbulence Mitigation', *Brain*, 44(0), pp. 767382–767382.
- [9] Sharifi, A. and Nobahari, H. (2016) 'Multiple model filters applied to wind model estimation for a fixed wing UAV', *Proceedings of 2016 7th International Conference on Mechanical and Aerospace Engineering, ICMAE 2016. IEEE*, pp. 109–115.